Investigation of Damage-Induced Ultrasound Signals Emitted by Fatigue Cracks in Steel Marine Structures

CECILIA SACCONE and LOTFOLLAH PAHLAVAN

ABSTRACT

In this paper, an investigation of the characterization of fatigue damage-induced signals by means of Acoustic Emission (AE) monitoring is presented. The objective is to establish a correlation between AE signals and fatigue crack growth data. To achieve this, small-scale fatigue experiments have been performed. The test consists of cyclic loading of standardized compact test (CT) specimens at room temperature. Damage-induced ultrasound signals were continuously measured using four AE transducers. The results suggest that AE signals emitted by fatigue crack growth from the initiation moment can be detected with a satisfactory signal-to-noise ratio. A multi-parameter analysis including amplitude, counts and hit rate of AE data in correlation with crack growth data was performed. Three stages of fatigue crack growth were identified, offering a basis for further damage characterisation using AE monitoring.

INTRODUCTION

Maritime steel structures are essential to the global shipping industry, offshore energy production and operations, and coastal infrastructures. Whether commercial port facilities, naval docks, offshore platforms, or specialized loading terminals, these steel infrastructures represent valuable national assets. These structures require significant investment to build and maintain. To ensure their operational safety and efficiency regular maintenance is essential so that failures can be prevented and reliability is guaranteed.

The primary failure mechanisms that can compromise the structural integrity of maritime steel structures are corrosion and fatigue [1] [2] [3].
Fatigue cracks often can develop in the vicinity of welded joints. Due to the complex geometry and limited accessibility of these areas, they can be difficult to detect and quantify [4].

Despite advances in non-destructive testing methods, fatigue crack detection in steel maritime structures remains challenging, with significant limitations in both accuracy and reliability. Current approaches to fatigue damage assessment primarily rely on a

Department of Marine and Transport Technology, Delft University of Technology, 2628CD, Delft, the Netherlands

combination of theoretical predictive models, such as S-N curves or fracture mechanics-based approaches, supplemented by in-situ strain measurements and operational load monitoring systems. Present damage assessment methods involve time-consuming and expensive processes, physically demanding and subjected to human errors [5] [6] [7]. Furthermore, no direct and continuous damage monitoring is performed on these structures.

Alternatively to the current methods, Structural Health Monitoring (SHM) systems enable continuous integrity assessments and facilitate predictive maintenance [8]. Within the SHM techniques, AE monitoring has already proven to be a valuable option for the integrity assessment of different structures (steel bridges, pipelines, offshore structures) [9] [10] [11]. In addition, it has other advantages; it can cover large areas with limited transducers, it has low implementation costs, and it is a passive method (no external excitation needed).

For the abovementioned reasons, AE can be considered a promising technique for continuous monitoring of ship structures. With Acoustic emission monitoring, it is possible to assess if a fatigue crack is active and propagating, playing an important role in the fatigue assessment of ships. By enabling more effective crack detection, AE monitoring can help reduce the risks associated with operations and environmental damage. In addition, AE monitoring supports predictive maintenance, which is essential for ships to optimize performance and extend service life.

AE signals can be directly correlated with either the emergence of new damage or the advancement of existing structural defects in materials. Each distinctive AE source that appears during fatigue damage development can be identified by specific parameters, including amplitude, count, and energy measurements. Different researchers have developed numerous methodologies for characterizing and monitoring AE signals throughout the damage evolution process [12] [13] [14] [15] [16] [17] [18], with a more exhaustive review of previous work available in [19].

Considering the limited applications of AE today in maritime steel structures, the potential is not fully realised, mainly due to outstanding complexities that have not yet been properly addressed. Among these complexities there is background noise interference, the presence of structural elements which additionally complicate the propagation of the ultrasound waves, and the lack of thorough investigation of the damage-induced AE signals. If these complexities could be successfully addressed, AE monitoring could be validly employed to assess the structural integrity of maritime structures. More specifically, consistent and general correlations between the AE and fatigue crack data have not yet been found. This could help to gain more insights into how different damage stages have different AE features. This could ultimately allow for the estimation of crack growth rate from AE measurement data.

In this paper, an investigation and characterisation of damage-induced AE signals emitted by fatigue cracks is carried out. A methodology for the characterization of fatigue-induced damage using AE monitoring is formulated. Small-scale experiments have been performed on CT steel specimens. AE transducers have been placed on the specimen during fatigue crack growth testing and have continuously recorded data. Simultaneously, direct crack growth measurement data have been collected using the direct current potential drop (DCPD) method. By doing this, an attempt has been made to identify the different damage source mechanisms from AE data. The outcomes of this investigation could help provide a starting point for the estimation of the remaining lifetime of ship structures.

METHODOLOGY

In thin-walled structures, damage-induced AE signals propagate as complex multimodal dispersive ultrasonic guided waves. These types of elastic waves propagate in multiple coexisting modes at different speeds [20] .

For a thin-walled steel specimen subjected to fatigue, Figure 1 shows schematically the ultrasound wave propagation recorded with an AE transducer. Given a damage-induced acoustic emission source indicated by *S*, which propagates through the steel medium *W*, the measured signal *P* at a sensor can be expressed in the frequency domain as the superposition of different modes *i*, plus a noise component *N*, with the following expression [21]:

$$P_j = \sum_{i=1}^{n} D_j W_i S + N \quad (1)$$

where D_j represents the transfer function of the sensor j and W_i is the transfer function . Every measured wave mode is the convolution of the source signal with the medium transfer function and the sensor transfer function. The noise component *N* in Equation (1) also includes the scatter and mode conversions of the non-dominant wave modes.

The investigation and characterization of damage-induced ultrasound signals emitted by fatigue cracks consist of focusing on the source term *S* of Equation (1).

For this, small-scale fatigue experiments have been performed in combination with AE monitoring to establish relationships between variations in the AE data and indications of active fatigue crack sources in the material.

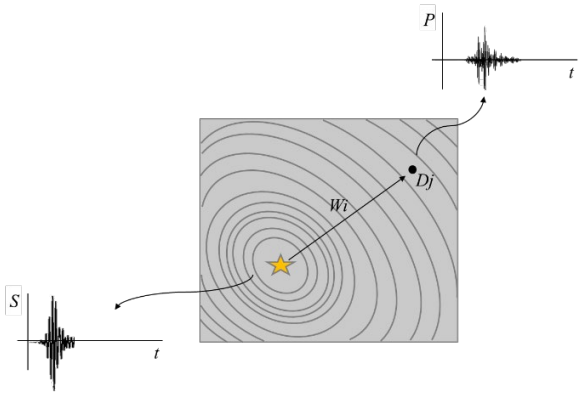

Figure 1. Damage-induced elastic wave emission in a steel plate.

EXPERIMENTAL SET-UP

The experimental setup was designed to apply fatigue loading on a steel specimen previously instrumented with AE monitoring sensors and a Direct Current Potential Drop (DCPD) system.

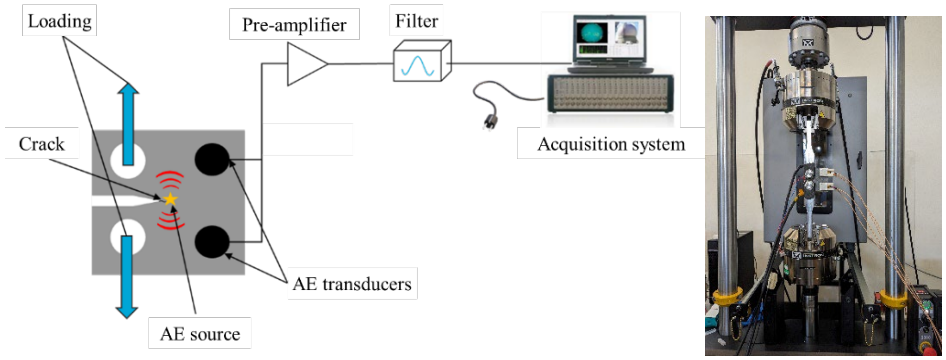

Figure 2. Schematic illustration of experimental set-up (left), and fatigue experimental set-up (right).

Figure 2 schematically illustrates the experimental set-up and equipment. The specimen is an ASTM standardized compact tension (CT) specimen of X65 steel. The CT specimen was cyclically tested using a biaxial Instron servo-hydraulic Tensile Testing Machine at room temperature with a peak load of 10 kN and a load ratio of 0.1. The specimen was equipped with four resonant AE transducers of the type R15alpha, which continuously measured ultrasound signals for the entire duration of the tests. The coupling of the four transducers was done with hot glue. The transducers were connected to AEPH5 preamplifiers (40 dB), and from there to an AMSY-6 data acquisition system. The sampling frequency was 10 MHz. The acquisition was hit-based and had a rearm and duration time of 250 µs and a pre-trigger period of 500 µs. A digital band-pass filter was applied, ranging from 95 kHz to 400 kHz. The acquisition threshold has been set to 40 dB based on an initial background noise assessment, ensuring that the AE signals were not masked by the machinery noise. According to the literature, these results comply with expected noise levels in the laboratory environment. Furthermore, to continuously measure the crack length, the specimen was also equipped with the direct current potential drop (DCPD) measurements (see Figure 3). On one side of the specimen, an acrylic paint layer (Figure 4, right) was present.

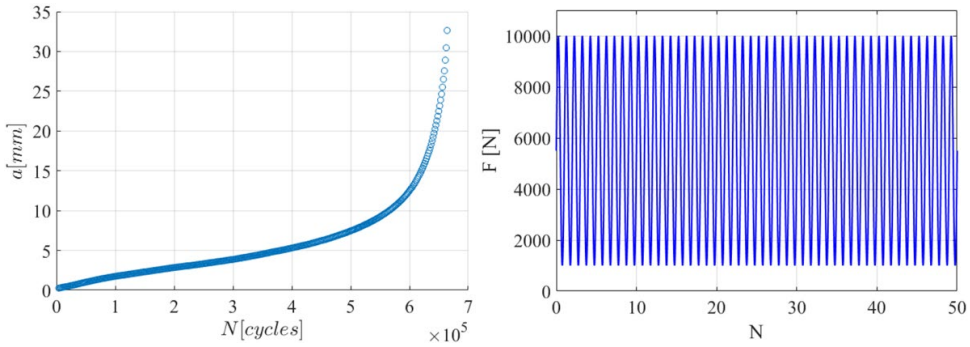

Figure 3. Crack size versus number of cycles (left); Sinusoidal loading versus first 50 cycles (right).

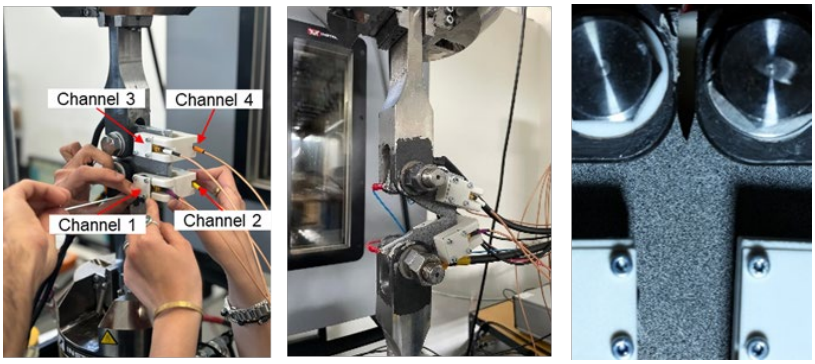

Figure 4. From left to right: Loaded specimen with the layout of the transducers; specimen after complete fracture; specimen close up with acrylic paint layer and AE transducers.

RESULTS AND DISCUSSION

The collected AE data was examined to gain insights into fatigue crack growth by attempting to identify correlations between AE characteristics and different stages of fatigue progression. The data from all four different sensors has been processed and analysed.

The specimen was tested from crack initiation until it failed after 660,000 constant amplitude load cycles. During the test, more than 20 million AE signals were collected. A filter based on SNR 2 was chosen in order to separate potential damage-induced signals from the background noise (continuous type signals). After applying SNR > 2, 4 million AE signals were analysed. Figure 5 shows the evolution of the cumulative number of AE signals as a function of load cycles for all four sensors (left), the total number of signals collected for each sensor during the duration of the test (center) and the variation of the hit-rate of AE signals as a function of load cycles for all four sensors (right).

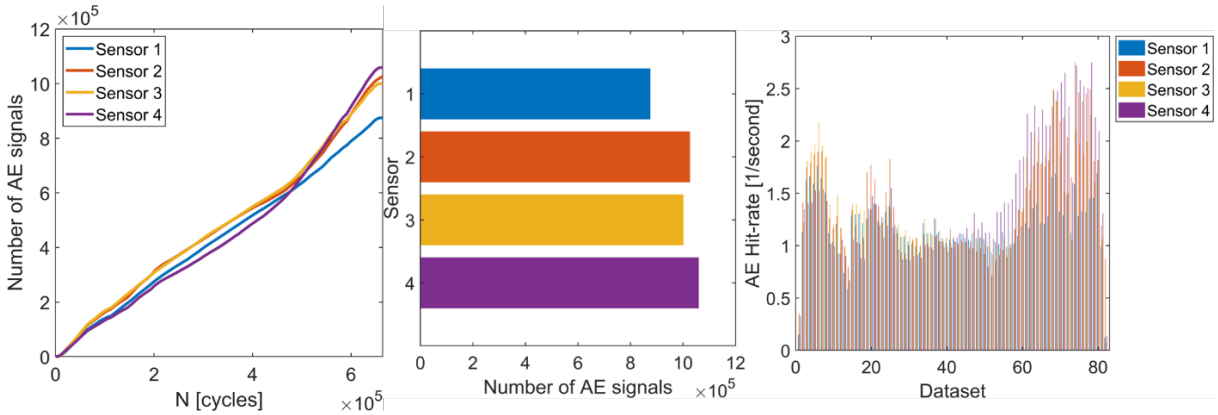

Figure 5. From left to right: Evolution of cumulative number of AE signals as a function of load cycles; recorded hits per second, variation of AE hit rate as a function of load cycles.

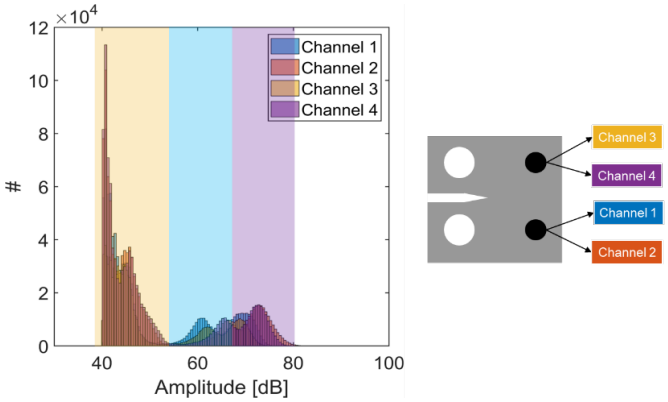

Figure 6. Amplitude distribution per sensor, breakdown into three amplitude clusters.

The trend of the cumulative number of AE signals increases with higher load cycles. The first part of the graph corresponding to the initial load cycles (beginning of the test) shows a rapid increase in the cumulative number of signals. This is followed by a slower rate in the middle part of the test. However, at the last stage, the cumulative trend results in a steeper curve more similar to the trend in the first stage. Looking at the hit-rate trend throughout the test, during the first stage of the test the hit rate is high up to 2 hits/second, possibly indicating crack initiation. Then the hit rate becomes lower during the middle part of the test, staying around 1 hit/second. In the last stage, the AE hit rate suddenly increases, reaching its highest values up to 3 hits/second, suggesting a higher crack growth rate and final failure of the specimen.

Further analysis was done by observing the amplitude distribution for the four AE sensors (Figure 6). More than 80% of the collected AE signals showed amplitudes between 40 and 50 dB. Sensors corresponding to channel 1 and channel 3 showed amplitudes around 10 dB lower than the sensors corresponding to channel 2 and 4 placed on the other side of the specimen. The pencil lead break (PLBs) tests showed a consistent 10 dB amplitude difference between the sensors on the two sides of the specimen. This difference is attributed to the presence of an acrylic paint layer on one side of the specimen. Furthermore, it is important to mention that all the sensors had hot glue coupling, which compared to the standard grease coupling, showed 20 dB lower amplitudes. This means that when corrected for the coupling effect, the amplitudes translate to a range of 60-100 dB for a gel-coupled situation.

The amplitude distribution in Figure 6 can be divided into three different amplitude clusters: I) amplitudes between 40 and 50 dB, II) amplitudes between 50 and 65 dB and III) amplitudes higher than 65 dB. The 65 dB boundary was selected based on an observed change in the slope of the amplitude distribution. For these three clusters, the cumulative number of AE signals, recorded hits per sensor and variation of AE hit/rate as a function of load cycles were calculated.

The first cluster contains the highest number of AE signals. The trends observed in the specific cluster closely resemble those of the total dataset (see Figure 5) and are therefore not separately illustrated in the figures.

The second and third clusters are shown in Figure 7. These clusters have significantly lower recorded AE signals but different cumulative and hit rate trends as functions of fatigue cycles compared to the first cluster. Looking at the evolution of the cumulative number of AE signals, for cluster II (solid lines), three changes in slope are visible, which can be attributed to the three different crack development stages

(initiation, growth and final failure). For cluster III (dashed lines), the cumulative number of AE signals shows a steep increase at the beginning until ¾ of the test duration, when it becomes almost stable until the end of the test. The bar chart of the number of recorded signals for the two clusters shows the same order of magnitude. The hit-rate data is presented only for channel 4, as the remaining channels exhibited similar patterns within the same cluster. For cluster II, the hit-rate shows values of 0.4 hits/second in the first stage of the test, possibly indicating crack initiation and then a sudden decrease to then increase towards the second half of the test until the end, going from 0 to 0.6 hits/second. This trend suggests a possible higher rate of crack growth before unstable crack growth and final failure of the specimen. For cluster III, the hit-rate shows higher values at the beginning of the test 0.4 hits/second, probably referring to crack initiation and then it gradually decreases towards the end of the test until 0.1 hits/second. In the second and third cluster, the hit rates generally display lower values compared to cluster one.

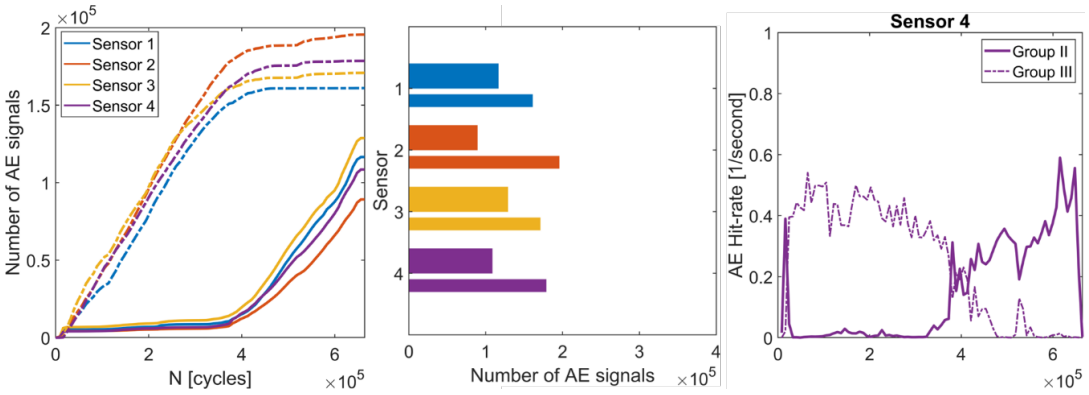

Figure 7. Evolution of cumulative number of AE signals (solid line: 55 to 65 dB; dashed line: 65 to 80 dB). Recorded hits per sensor (thicker bars: 55 to 65 dB; thinner bars: 65 to 80 dB); Variation of AE hit rate as a function of cycles for sensor 4 (solid line: 55 to 65 dB; dashed line: 65 to 80 dB).

CONCLUSIONS

An investigation of the AE signals generated during fatigue crack growth was performed using small-scale fatigue experiments. At the end of the tests, after 660,000 constant-amplitude cycles, over 20 million AE signals were recorded and processed from the X65 CT specimen. This analysis suggests three different clusters based on signal amplitude. Each of the clusters shows different trends for the hit rate and the cumulative number of signals, which could potentially be associated with different fatigue crack growth stages. A promising agreement was observed between crack size and the cumulative number of signals in the 55-65 dB range across fatigue cycles. Further analysis could help identify correlations between acoustic emission data and fatigue crack measurements obtained experimentally. This could be used as a starting point for damage characterisation in ship structures using AE monitoring. Further assessment could involve parametric analysis, focusing on the frequency and energy content of the signals within each cluster.

ACKNOWLEDGEMENTS

The authors would like to acknowledge The Netherlands Organization for Scientific Research (NWO) and project partners for co-funding and technical support.

REFERENCES

1. U. O. Akpana, T. Kokoa, B. Ayyubb and T. Dunbara, "Risk assessment of aging ship hull structures in the presence of corrosion and fatigue," *Marine Structures,* vol. 15, pp. 211-231, 2002.
2. Y. Dong and D. M. Frangopol, "Risk-informed life-cycle optimum inspection and maintenance of ship structures considering corrosion and fatigue," *Ocean Engineering,* vol. 101, pp. 161-171, 2015.
3. E. H. Cramer, R. Loseth and K. Olaisen, "Fatigue Assessment of Ship Structures," *Marine structures,* vol. 8, pp. 359 - 383, 1995.
4. R. Hageman, *Uncertainty quantification of fatigue design loads when compared with in-service,* 2022.
5. R. A. Votsis, C. Michailides, E. A. Tantele and T. Onoufriou, "Review of Technologies for Monitoring the Performance of Marine Structures," in *International Ocean and Polar Engineering Conference*, 2018.
6. J. Zhang, W.-H. Kang, K. Sun and F. Liu, "Reliability-Based Serviceability Limit State Design of a Jacket Substructure for an Offshore Wind Turbine," *energies ,* 2019.
7. Committee V.7, "ISSC report," 2022.
8. M. G. R. Sause and E. Jasiūnienė, Eds., Structural Health Monitoring Damage Detection Systems for Aerospace, 2021.
9. N. H. Faisal, M. G. Droubi and J. A. Steel, "Corrosion monitoring of offshore structures using acoustic emission sensors," *A journal of the Institute of Corrosion,* 2017.
10. ASTM International , *E1316-13c Standard Terminology for Nondestructive Examinations,* 2013.
11. F. Riccioli, Ø. Gabrielsen, I. S. Høgsæt, P. S. Barros and L. Pahlavan, "Corrosion-fatigue damage identification in submerged mooring chain links using remote acoustic emission monitoring," *Marine Structures,* 2024.
12. D. Aggelis, E. Kordatos and T. Matikas, "Acoustic emission for fatigue damage characterization in metal plates," *Mechanics Research Communications,* vol. 38, no. 2, pp. 106-110, 2011.
13. H. Bi, H. Li, W. Zhang, L. Wang, Q. Zhang, S. Cao and I. Toku-Gyamerah, "Evaluation of the acoustic emission monitoring method for stress corrosion cracking on aboveground storage tank floor steel," *International Journal of Pressure Vessels and Piping,* vol. 179, 2020.
14. M. Chai, X. Hou, Z. Zhang and Q. Duan, "Identification and prediction of fatigue crack growth under different stress ratios using acoustic emission data," *International Journal of Fatigue,* vol. 160, 2022.
15 M. Chai, C. Lai, W. Xu, Q. Duan, Z. Zhang and Y. Song, "Characterization of Fatigue Crack Growth Based on Acoustic Emission Multi-Parameter Analysis," *materials,* 2022.
16. H. Chang, E. Han, J. Q. Wang and W. Ke, "Acoustic emission study of corrosion fatigue crack propagation mechanism for LY12CZ and 7075-T6 aluminum alloys," *Journal of Material Science,* 2005.
17. G. Du, J. Li, W. Wang, C. Jiang and S. Song, "Detection and characterization of stress-corrosion cracking on 304 stainless steel by electrochemical noise and acoustic emission techniques," *Corrosion Science,* vol. 53, no. 9, pp. 2918-2926, 2011.
18. Z. Han, H. Luo, J. Cao and H. Wang, "Acoustic emission during fatigue crack propagation in a micro-alloyed steel and welds," *Materials Science and Engineering,* vol. 528, no. 25-26, pp. 7751-7756, 2011.
19. F. Riccioli, S. Alkhateeb, A. Mol and L. Pahlavan, "Feasibility assessment of non-contact acoustic emission monitoring of corrosion-fatigue damage in submerged steel structures," *Ocean Engineering,* 2024.
20. P. L. Pahlavan, J. Paulissen, R. Pijpers, H. Hakkesteegt and R. Jansen, *Acoustic Emission Health Monitoring of Steel Bridges,* Nantes, France: EWSHM - 7th European Workshop on Structural Health Monitoring, 2014.
21. B. Scheeren, M. L. Kaminski and L. Pahlavan, "Acoustic emission monitoring of naturally developed damage in large-scale low-speed roller bearings," *Structural Health Monitoring,* 2023.